

RESEARCH PAPER

Nitrogen demand, availability, and acquisition strategy control plant responses to elevated CO₂

Evan A. Perkowski^{*}, Ezinwanne Ezekannagha, and Nicholas G. Smith

Department of Biological Sciences, Texas Tech University, Lubbock, TX 79409, USA

* Correspondence: evan.a.perkowski@ttu.edu

Received 17 December 2024; Editorial decision 10 March 2025; Accepted 11 March 2025

Editor: Alistair Rogers, Lawrence Berkeley National Laboratory, USA

Abstract

Plants respond to increasing atmospheric CO₂ concentrations by reducing leaf nitrogen content and photosynthetic capacity—patterns that correspond with increased net photosynthesis and growth. Despite the longstanding notion that nitrogen availability regulates these responses, eco-evolutionary optimality theory posits that leaf-level responses to elevated CO₂ are driven by leaf nitrogen demand for building and maintaining photosynthetic enzymes and are independent of nitrogen availability. In this study, we examined leaf and whole-plant responses of *Glycine max* L. (Merr) subjected to full-factorial combinations of two CO₂, two inoculation, and nine nitrogen fertilization treatments. Nitrogen fertilization and inoculation did not alter leaf photosynthetic responses to elevated CO₂. Instead, elevated CO₂ decreased the maximum rate of ribulose-1,5-bisphosphate oxygenase/carboxylase (Rubisco) carboxylation more strongly than it decreased the maximum rate of electron transport for ribulose-1,5-bisphosphate (RuBP) regeneration, increasing net photosynthesis by allowing rate-limiting steps to approach optimal coordination. Increasing fertilization enhanced positive whole-plant responses to elevated CO₂ due to increased below-ground carbon allocation and nitrogen uptake. Inoculation with nitrogen-fixing bacteria did not influence plant responses to elevated CO₂. These results reconcile the role of nitrogen availability in plant responses to elevated CO₂, showing that leaf photosynthetic responses are regulated by leaf nitrogen demand while whole-plant responses are constrained by nitrogen availability.

Keywords: Acclimation, biomass, eco-evolutionary optimality, growth chamber, least-cost theory, optimal coordination, photosynthesis, plant functional ecology, resource optimization.

Introduction

Complex carbon and nitrogen cycles regulate terrestrial ecosystems. Terrestrial biosphere models that incorporate coupled carbon and nitrogen cycles must accurately represent the processes and interactions governing these cycles across different environmental scenarios to simulate carbon and nitrogen fluxes reliably (Hungate *et al.*, 2003; Prentice *et al.*, 2015; Davies-Barnard *et al.*, 2020; Kou-Giesbrecht *et al.*, 2023). However,

uncertainties remain regarding how nitrogen availability and plant nitrogen acquisition strategy influences leaf and whole-plant responses to increasing atmospheric CO₂ concentrations, leading to divergent predictions of future carbon and nitrogen pools and fluxes across models (Arora *et al.*, 2020; Davies-Barnard *et al.*, 2020, 2022; Meyerholt *et al.*, 2020; Stocker *et al.*, 2025).

Research spanning several decades has documented consistent trends in leaf and whole-plant responses to elevated CO₂. At the leaf level, C₃ plants exhibit increased net photosynthesis rates that correspond with reduced leaf nitrogen content, stomatal conductance, and photosynthetic capacity when grown under elevated CO₂ compared with ambient conditions (Curtis, 1996; Drake *et al.*, 1997; Nakano *et al.*, 1997; Medlyn *et al.*, 1999; Ainsworth *et al.*, 2002; Ainsworth and Long, 2005; Bernacchi *et al.*, 2005; Ainsworth and Rogers, 2007; Crous *et al.*, 2010; Lee *et al.*, 2011; Pastore *et al.*, 2019; Poorter *et al.*, 2022; Cui *et al.*, 2023; Stocker *et al.*, 2025). At the whole-plant level, CO₂ enrichment increases total leaf area, promoting greater primary productivity and biomass accumulation (Coleman *et al.*, 1993; Makino *et al.*, 1997; Ainsworth *et al.*, 2002; Ainsworth and Rogers, 2007; Finzi *et al.*, 2007; Poorter *et al.*, 2022). Some studies suggest that elevated CO₂ increases below-ground carbon allocation and root:shoot ratios (Iversen *et al.*, 2008; Iversen, 2010; Nie *et al.*, 2013; Stocker *et al.*, 2025), although these responses are not consistently observed (Luo *et al.*, 1994; Poorter *et al.*, 2022) and are highly variable across experiments (Stocker *et al.*, 2025).

Two hypotheses—the nitrogen limitation hypothesis and the eco-evolutionary optimality hypothesis—offer contrasting views on how nitrogen availability shapes plant responses to elevated CO₂. The nitrogen limitation hypothesis posits that nitrogen availability constrains plant responses to elevated CO₂, as nitrogen availability limits net primary productivity and influences the magnitude of the terrestrial carbon sink (Vitousek and Howarth, 1991; LeBauer and Treseder, 2008; Sigurdsson *et al.*, 2013; Wieder *et al.*, 2015). Elevated CO₂ increases whole-plant nitrogen demand for building new tissues, which may lead to greater nitrogen limitation of net primary productivity without additional ecosystem nitrogen inputs (Luo *et al.*, 2004). Thus, increased nitrogen availability should amplify the positive effects of elevated CO₂ on net primary productivity and biomass accumulation, provided that nitrogen availability exceeds whole-plant demand. Free-air CO₂ enrichment studies offer mixed support for this hypothesis, with some studies supporting its predictions (Reich *et al.*, 2006; Norby *et al.*, 2010) and others not (Finzi *et al.*, 2006; Moore *et al.*, 2006; Liang *et al.*, 2016). The hypothesis also implies that reductions in leaf nitrogen content and photosynthetic capacity under elevated CO₂ are linked to ecosystem nitrogen limitation, as positive correlations between soil nitrogen availability, leaf nitrogen content, and photosynthetic capacity are common (Field and Mooney, 1986; Evans, 1989). However, evidence shows that reductions in leaf nitrogen content and photosynthetic capacity under elevated CO₂ are often decoupled from changes in nitrogen availability (Crous *et al.*, 2010; Lee *et al.*, 2011; Pastore *et al.*, 2019), indicating that other factors, such as demand for building and maintaining photosynthetic tissues, might play an important role in determining leaf-level responses.

Conversely, the eco-evolutionary optimality hypothesis asserts that leaf-level demand to build and maintain photosynthetic enzymes drives leaf-level photosynthetic responses to elevated CO₂ and that these responses are independent of nitrogen availability (Harrison *et al.*, 2021). The hypothesis combines photosynthetic least-cost (Wright *et al.*, 2003; Prentice *et al.*, 2014) and optimal coordination (Chen *et al.*, 1993; Maire *et al.*, 2012) theories, suggesting that elevated CO₂ down-regulates the maximum rate of Rubisco carboxylation (V_{cmax}) more strongly than the maximum rate of electron transport for ribulose-1,5-bisphosphate (RuBP) regeneration (J_{max}). The down-regulation in V_{cmax} is attributed to increased CO₂ availability under elevated CO₂, which enhances Rubisco affinity for carboxylation relative to oxygenation and reduces demand for building and maintaining additional Rubisco enzymes (Bazzaz, 1990; Dong *et al.*, 2022). The eco-evolutionary optimality hypothesis predicts that plants optimize leaf nitrogen allocation to photosynthetic capacity to use available light efficiently while avoiding overinvestment in Rubisco, which has high nitrogen and energetic costs to build and maintain (Evans, 1989; Sage, 1994; Evans and Clarke, 2019). This strategy enhances photosynthetic nitrogen-use efficiency and allows increased net photosynthesis rates to be achieved by increasing the co-limitation of net photosynthesis rates by Rubisco carboxylation and electron transport for RuBP regeneration (Chen *et al.*, 1993; Maire *et al.*, 2012; Wang *et al.*, 2017; Smith *et al.*, 2019). Empirical evidence supports this hypothesis (Crous *et al.*, 2010; Lee *et al.*, 2011; Smith and Keenan, 2020; Harrison *et al.*, 2021; Dong *et al.*, 2022; Cui *et al.*, 2023), though few studies have connected these patterns with concurrently measured whole-plant responses.

While the eco-evolutionary optimality hypothesis predicts that leaf-level photosynthetic responses are independent of nitrogen availability, it acknowledges that nitrogen availability may regulate whole-plant responses to elevated CO₂. The hypothesis suggests that the optimal whole-plant response to elevated CO₂ involves allocating surplus nitrogen not needed to satisfy leaf-level demand to build and maintain photosynthetic enzymes toward constructing additional optimally coordinated leaves and other plant organs. Furthermore, the hypothesis implies that optimal resource allocation to photosynthetic capacity leads to nitrogen savings at the leaf level, maximizing resource allocation to support whole-plant growth (Smith *et al.*, 2024). Thus, the extent to which plant responses to elevated CO₂ align with the nitrogen limitation or eco-evolutionary optimality hypothesis may be a question of scale, with leaf-level responses driven by leaf-level photosynthetic demand and whole-plant responses regulated by nitrogen availability.

Plant nitrogen acquisition strategy complicates the role of nitrogen availability in plant responses to elevated CO₂. Plants use a variety of strategies to acquire nitrogen, including direct uptake from the soil or through symbiotic relationships with mycorrhizal fungi and nitrogen-fixing bacteria (Barber, 1962; Gutschick, 1981;

Smith and Read, 2008). The carbon costs associated with nitrogen acquisition vary among species with different acquisition strategies and depend on environmental factors such as atmospheric CO₂, temperature, light availability, and nutrient availability (Fisher et al., 2010; Brzostek et al., 2014; Terrer et al., 2018; Allen et al., 2020; Perkowski et al., 2021; Lu et al., 2022; Peng et al., 2023; Perkowski et al., 2024; Cheaib et al., 2025). Carbon costs to acquire nitrogen can influence nitrogen uptake and, in turn, affect nitrogen allocation to different plant organs, investment in photosynthetic tissues, and biomass accumulation (Terrer et al., 2018; Perkowski et al., 2021, 2024; Waring et al., 2023). Therefore, considering the nitrogen acquisition strategy is important when examining plant responses to elevated CO₂ across nitrogen availability gradients, especially because whole-plant responses to elevated CO₂ are often positively correlated with nitrogen uptake (Feng et al., 2015; Stocker et al., 2025). However, few studies account for plant acquisition strategy when considering the role of nitrogen availability in plant responses to elevated CO₂ (Terrer et al., 2016, 2018; Smith and Keenan, 2020). Despite this, emerging evidence suggests that acquisition strategies with lower carbon costs for nitrogen acquisition may mitigate nitrogen limitation at the whole-plant level, though leaf-level responses remain less clear (Terrer et al., 2018; Smith and Keenan, 2020).

Here, we examined whether plant responses to elevated CO₂ align with the nitrogen limitation or eco-evolutionary optimality hypothesis and assessed how the nitrogen acquisition strategy modifies these responses. Using a growth chamber experiment, we grew *Glycine max* L. (Merr.) seedlings under two CO₂ concentrations (420 ppm and 1000 ppm CO₂), two nitrogen acquisition strategies (with and without *Bradyrhizobium japonicum*), and nine soil nitrogen fertilization treatments (ranging from 0 ppm to 630 ppm N) in a full-factorial design. We used this experimental setup to test the following hypotheses.

- (i) Following the eco-evolutionary optimality hypothesis, leaf photosynthetic responses to elevated CO₂ will be independent of nitrogen fertilization and inoculation treatment. Instead, elevated CO₂ will decrease V_{cmax} more than J_{max} , increasing the ratio of J_{max} to V_{cmax} . This response will increase net photosynthesis rates under growth CO₂ conditions by allowing rate-limiting steps to approach optimal coordination while enhancing photosynthetic nitrogen-use efficiency.
- (ii) Following the nitrogen limitation hypothesis, increasing nitrogen fertilization will enhance the positive effects of elevated CO₂ on total leaf area and total biomass. This response will be due to increased below-ground carbon allocation and nitrogen uptake, and with increasing nitrogen fertilization that will be stronger under elevated CO₂. Biomass responses to elevated CO₂ will be driven by a greater increase in below-ground biomass than above-ground biomass, as plants will invest in resource acquisition strategies to meet the increased whole-plant nitrogen demand for building new tissues.

- (iii) Following the nitrogen limitation hypothesis, inoculation with nitrogen-fixing bacteria will enhance positive whole-plant responses to elevated CO₂. These responses will be strongest under low nitrogen availability, where inoculated plants will invest in nitrogen uptake through symbiotic nitrogen fixation over more costly direct uptake pathways. However, these patterns will diminish with increasing nitrogen fertilization as plants acquire more nitrogen through increasingly less costly direct uptake pathways.

Materials and methods

Seed treatments and experimental design

Glycine max L. (Merr) seeds (Territorial Seed Co., Cottage Grove, OR, USA) were planted in 144 surface-sterilized pots (NS-600, 6 liter capacity; Nursery Supplies, Orange, CA, USA) containing a steam-sterilized 70:30 v:v mix of *Sphagnum* peat moss (Premier Horticulture, Quakertown, PA, USA) to sand (Pavestone, Atlanta, GA, USA). Before planting, all *G. max* seeds were surface-sterilized in 2% sodium hypochlorite for 3 min, followed by three 3 min washes with ultrapure water (MilliQ 7000; MilliporeSigma, Burlington, MA, USA). Subsets of surface-sterilized seeds were inoculated with *B. japonicum* (Verdesian N-Dure™ Soybean, Cary, NC, USA) in a slurry following the manufacturer's recommendations (3.12 g of inoculant and 241 g of ultrapure water per 1 kg of seed).

Seventy-two pots were randomly planted using surface-sterilized seeds inoculated with *B. japonicum*, while the remaining 72 pots were planted using surface-sterilized uninoculated seeds. Thirty-six pots in each inoculation treatment were placed in one of two atmospheric CO₂ treatments (420 μmol mol⁻¹ CO₂ or 1000 μmol mol⁻¹ CO₂). CO₂ treatments were decided based on current ambient CO₂ concentrations and projections from the Intergovernmental Panel on Climate Change indicating that CO₂ concentrations could surpass 1000 ppm by 2100 under the Shared Socioeconomic Pathway 5–8.5 (IPCC, 2021). Plants in each unique inoculation×CO₂ treatment combination received one of nine nitrogen fertilization treatments equivalent to 0 (0 mM), 35 (2.5 mM), 70 (5 mM), 105 (7.5 mM), 140 (10 mM), 210 (15 mM), 280 (20 mM), 350 (25 mM), or 630 ppm (45 mM) N. This experimental setup resulted in four replicates per unique inoculation×CO₂×nitrogen fertilization treatment combination. Nitrogen fertilization treatments were created using a modified Hoagland's solution (Hoagland and Arnon, 1950) designed to keep concentrations of all other macronutrients and micronutrients equivalent across treatments (Supplementary Table S1). Plants received the same nitrogen fertilization treatment twice per week in 150 ml doses as topical agents to the soil surface. Plants were well watered between fertilization doses to ensure that physiology and growth were not limited by water availability.

Growth chamber conditions

Plants were randomly placed in one of six calibrated Percival LED-41L2 growth chambers (Percival Scientific Inc., Perry, IA, USA) over two experimental iterations due to chamber space limitation. The first iteration included all plants grown under elevated CO₂, while the second included all plants grown under ambient CO₂. Average (±SD) CO₂ concentrations across chambers throughout the experiment were 439±5 μmol mol⁻¹ CO₂ for the ambient treatment and 989±4 μmol mol⁻¹ CO₂ for the elevated treatment. Each experimental iteration lasted 7 weeks, which was sufficient for plants to grow through the majority of their vegetative growth phase without evidence of reproduction.

Daytime growth conditions were simulated using a 16 h photoperiod, with incoming light radiation set to chamber maximum (mean \pm SD: $1230 \pm 12 \mu\text{mol m}^{-2} \text{s}^{-1}$ across chambers), air temperature to 25 °C, and relative humidity set 50%. This daylength allowed plants to maximize vegetative growth across the 7 week experiment while minimizing the onset of reproduction. The remaining 8 h period simulated night-time growing conditions, with incoming light radiation set to $0 \mu\text{mol m}^{-2} \text{s}^{-1}$, chamber temperature to 17 °C, and relative humidity to 50%. Transitions between daytime and night-time growing conditions were simulated by ramping incoming light radiation in 45 min increments and temperature in 90 min increments over 3 h (Supplementary Table S2).

Plants grew under average (\pm SD) daytime light intensity of $1049 \pm 27 \mu\text{mol m}^{-2} \text{s}^{-1}$, including ramping periods. In the elevated CO_2 iteration, plants grew under 24.0 ± 0.2 °C during the day, 16.4 ± 0.8 °C during the night, and $51.6 \pm 0.4\%$ relative humidity. In the ambient CO_2 iteration, plants grew under 23.9 ± 0.2 °C during the day, 16.0 ± 1.4 °C during the night, and $50.3 \pm 0.2\%$ relative humidity. Any differences in climate conditions across the six chambers were accounted for by shuffling the same group of plants throughout the growth chambers. This process was done by iteratively moving the group of plants on the top rack of a chamber to the bottom rack of the same chamber while simultaneously moving the group of plants on the bottom rack of a chamber to the top rack of the adjacent chamber. Plants were moved within and across chambers daily during each experiment iteration.

Leaf gas exchange measurements

Leaf gas exchange measurements were collected in all plants ($n=144$ individuals) during the seventh week of development, before the onset of reproduction. All gas exchange measurements were collected on the center leaflet of the most recent fully expanded trifoliate leaflet set using LI-6800 portable photosynthesis machines configured with a 6800-01A fluorometer head and 6 cm^2 aperture (LI-COR Biosciences, Lincoln, NE, USA). Specifically, net photosynthesis rates (A_{net} ; $\mu\text{mol m}^{-2} \text{s}^{-1}$), stomatal conductance rates (g_{sw} ; $\text{mol m}^{-2} \text{s}^{-1}$), and intercellular CO_2 concentrations (C_i ; $\mu\text{mol mol}^{-1}$) were measured across a range of atmospheric CO_2 concentrations (i.e. an A_{net}/C_i curve) using the Dynamic Assimilation™ Technique. The Dynamic Assimilation™ Technique corresponds well with traditional steady-state A_{net}/C_i curves in *G. max* (Saathoff and Welles, 2021; Tejera-Nieves *et al.*, 2024). A_{net}/C_i curves were generated along a reference CO_2 ramp down from $420 \mu\text{mol mol}^{-1} \text{CO}_2$ to $20 \mu\text{mol mol}^{-1} \text{CO}_2$, followed by a ramp up from $420 \mu\text{mol mol}^{-1} \text{CO}_2$ to $1620 \mu\text{mol mol}^{-1} \text{CO}_2$ after a 90 s wait period at $420 \mu\text{mol mol}^{-1} \text{CO}_2$. The ramp rate for each curve was set to $200 \mu\text{mol mol}^{-1} \text{min}^{-1}$, logging every 5 s, generating 96 data points per response curve. All A_{net}/C_i curves were conducted after A_{net} and g_{sw} stabilized in an LI-6800 cuvette set to a 500 mol s^{-1} flow rate, 10 000 rpm mixing fan speed, 1.5 kPa vapor pressure deficit, 25 °C leaf temperature, $2000 \mu\text{mol m}^{-2} \text{s}^{-1}$ incoming light radiation, and initial reference CO_2 concentration set to $420 \mu\text{mol mol}^{-1}$.

Snapshot A_{net} measurements were extracted from each A_{net}/C_i curve, at both a common CO_2 concentration, $420 \mu\text{mol mol}^{-1} \text{CO}_2$ ($A_{\text{net},420}$; $\mu\text{mol m}^{-2} \text{s}^{-1}$), and growth CO_2 concentration, $420 \mu\text{mol mol}^{-1} \text{CO}_2$ and $1000 \mu\text{mol mol}^{-1} \text{CO}_2$ ($A_{\text{net},\text{gc}}$; $\mu\text{mol m}^{-2} \text{s}^{-1}$). We quantified $A_{\text{net},420}$ to gauge the relative investment in photosynthetic tissues between treatment combinations, and $A_{\text{net},\text{gc}}$ to quantify photosynthetic performance between treatment combinations. Dark respiration (R_d ; $\mu\text{mol m}^{-2} \text{s}^{-1}$) measurements were collected on the same leaflet used to generate A_{net}/C_i curves following at least a 30 min period of darkness. Dark respiration measurements were collected on a 5 s log interval for 60 s after the leaf stabilized in an LI-6800 cuvette set to a 500 mol s^{-1} flow rate, 10 000 rpm mixing fan speed, 1.5 kPa vapor pressure deficit, 25 °C leaf temperature, and $420 \mu\text{mol mol}^{-1}$ reference CO_2 concentration (regardless of CO_2 treatment), with incoming light radiation set to $0 \mu\text{mol m}^{-2} \text{s}^{-1}$. A single

R_d value was determined for each leaflet by calculating the mean R_d value across the logging interval.

A/C_i curve fitting and parameter estimation

A_{net}/C_i curves were fit using the 'fitaci' function in the 'plantecophys' R package (Duursma, 2015). This function estimates the apparent maximum rate of Rubisco carboxylation (V_{cmax} ; $\mu\text{mol m}^{-2} \text{s}^{-1}$) and apparent maximum rate of electron transport for RuBP regeneration (J_{max} ; $\mu\text{mol m}^{-2} \text{s}^{-1}$) based on the Farquhar *et al.* (1980) biochemical model of C_3 photosynthesis. Triose phosphate utilization (TPU) limitation was included as an additional rate-limiting step after visually observing clear TPU limitation for most curves. All curve fits included measured dark respiration values. As A_{net}/C_i curves were generated using a common leaf temperature (25 °C), curves were fit using Michaelis–Menten coefficients for Rubisco affinity for CO_2 (K_c ; $\mu\text{mol mol}^{-1}$) and O_2 (K_o ; mmol mol^{-1}), and the CO_2 compensation point (Γ^* ; $\mu\text{mol mol}^{-1}$) reported in Bernacchi *et al.* (2001). Specifically, K_c was set to $404.9 \mu\text{mol mol}^{-1}$, K_o was set to $278.4 \mu\text{mol mol}^{-1}$, and Γ^* was set to $42.75 \mu\text{mol mol}^{-1}$. V_{cmax} , J_{max} , and R_d estimates are referenced throughout the rest of the paper as $V_{\text{cmax}25}$, $J_{\text{max}25}$, and R_{d25} .

Leaf trait measurements

The leaflet used for A_{net}/C_i curves and dark respiration measurements was harvested immediately following gas exchange measurements. Images of each focal leaflet were curated using a flat-bed scanner to determine fresh leaf area using the 'LeafArea' R package (Katabuchi, 2015), which automates leaf area calculations using ImageJ software (Schneider *et al.*, 2012). Post-processed images were visually assessed to check against errors in the automation process. Each focal leaflet was dried at 65 °C for at least 48 h, weighed, and ground until homogenized. Leaf mass per area (M_{area} ; g m^{-2}) was calculated as the ratio of dry leaflet biomass to fresh leaflet area. Leaf nitrogen content (N_{mass} ; gN g^{-1}) was quantified using a subsample of ground and homogenized leaflet tissue through elemental combustion (Costech-4010, Costech, Inc., Valencia, CA, USA). Leaf nitrogen content per unit leaf area (N_{area} ; gN m^{-2}) was calculated by multiplying N_{mass} and M_{area} . Photosynthetic nitrogen-use efficiency (PNUE_{gc} ; $\mu\text{mol CO}_2 \text{g}^{-1} \text{N s}^{-1}$) was estimated as the ratio of $A_{\text{net},\text{gc}}$ to N_{area} .

Chlorophyll content was extracted from a second leaflet in the same trifoliate leaf set as the leaf used to generate A_{net}/C_i curves. A cork borer was used to punch between three and five 0.6 cm^2 disks from the leaflet. Images of each set of leaflet disks were curated using a flat-bed scanner to determine wet leaf area using the 'LeafArea' R package (Katabuchi, 2015). Leaflet disks were shuttled into a test tube containing 10 ml of DMSO, vortexed, and incubated at 65 °C for 120 min (Barnes *et al.*, 1992). Incubated test tubes were vortexed again before being loaded in 150 μl triplicate aliquots to a 96-well plate. DMSO was loaded in each plate as a single 150 μl triplicate aliquot and used as a blank. Absorbance measurements at 649 nm (A_{649}) and 665 nm (A_{665}) were recorded using a plate reader (Biotek Synergy H1; Biotek Instruments, Winooski, VT, USA), with triplicate measurements averaged and corrected by the mean of the blank absorbance value. Blank-corrected absorbance values were used to estimate Chl *a* ($\mu\text{g ml}^{-1}$) and Chl *b* ($\mu\text{g ml}^{-1}$) following equations from Wellburn (1994):

$$\text{Chl}_a = 12.19A_{665} - 3.45A_{649} \quad (1)$$

and

$$\text{Chl}_b = 21.99A_{649} - 5.32A_{665} \quad (2)$$

Chl *a* and Chl *b* were converted to mmol ml⁻¹ using the molar masses of Chl *a* (893.51 g mol⁻¹) and Chl *b* (907.47 g mol⁻¹), then added together to calculate the total chlorophyll content in DMSO extractant (mmol ml⁻¹). Total chlorophyll content (mmol) was determined by multiplying the total chlorophyll content in DMSO by the volume of DMSO (10 ml). Area-based chlorophyll content (Chl_{area} ; mmol m⁻²) was calculated by dividing the total chlorophyll content by the total area of the leaflet disks.

Whole-plant measurements

All individuals were harvested, and the biomass of major organ types (leaves, stems, roots, and nodules when present) were separated immediately following gas exchange measurements during the seventh week of development. Fresh leaf area of all harvested leaflets was measured using an LI-3100C (LI-COR Biosciences). Total fresh leaf area (cm²) was calculated as the sum of all leaflet areas, including those used for gas exchange and chlorophyll extractions. Harvested material was separately dried in an oven set to 65 °C for at least 48 h to a constant mass, weighed, and then ground to homogeneity. Leaves and root nodules were ground using a mortar and pestle, while stems and roots were ground using an E3300 Single Speed Mini Cutting Mill (Eberbach Corp., MI, USA). Total biomass (g) was calculated as the sum of dry leaf, stem, root, and root nodule biomass. Carbon and nitrogen content was measured for each organ type through elemental combustion (Costech-4010, Costech, Inc., Valencia, CA, USA) using ground and homogenized organ tissue subsamples. The ratio of root nodule biomass to root biomass was calculated as an indicator of plant investment toward nitrogen fixation relative to other uptake pathways (e.g. direct uptake). The root:shoot ratio (unitless) was calculated as the ratio of below-ground biomass (root and root nodule biomass) to shoot biomass (leaf and stem biomass). Leaf, stem, and root mass fractions were calculated as the dry biomass of each respective organ per unit total biomass (g g⁻¹ in all cases).

Below-ground biomass carbon costs to acquire nitrogen were quantified as the ratio of below-ground biomass carbon to whole-plant nitrogen biomass (g C g N⁻¹) (Perkowski *et al.*, 2021). Below-ground biomass carbon (g C) was calculated as the sum of root and root nodule carbon biomass. Root carbon biomass and root nodule carbon biomass were calculated as the product of the organ biomass and the respective organ carbon content. Whole-plant nitrogen biomass (g N) was calculated as the sum of total leaf, stem, root, and root nodule nitrogen biomass. Leaf, stem, root, and root nodule nitrogen biomass was calculated as the product of the organ biomass and respective organ nitrogen content. This calculation does not account for additional carbon costs associated with respiration, root exudation, or root turnover, and may underestimate carbon costs to acquire nitrogen (Perkowski *et al.*, 2021).

Statistical analyses

Uninoculated plants with substantial root nodule formation (root nodule biomass:root biomass values >0.05 g g⁻¹) were removed from analyses following the assumption that plants were incompletely sterilized or contaminated. This decision resulted in the removal of 16 plants from the analysis: two plants in the elevated CO₂ treatment that received 35 ppm N, three plants in the elevated CO₂ treatment that received 70 ppm N, one plant in the elevated CO₂ treatment that received 210 ppm N, two plants in the elevated CO₂ treatment that received 280 ppm N, two plants in the ambient CO₂ treatment that received 0 ppm N, three plants in the ambient CO₂ treatment that received 70 ppm N, two plants in the ambient CO₂ treatment that received 105 ppm N, and one plant in the ambient CO₂ treatment that received 280 ppm N. A summary of the replication scheme after these individuals were removed is included in Supplementary Tables S3 and S4).

A series of linear mixed-effects models were built to investigate the impacts of CO₂ concentration, nitrogen fertilization, and inoculation

on *G. max* leaf nitrogen content, leaf gas exchange, total leaf area, biomass, biomass allocation, and plant investment in symbiotic nitrogen fixation. All models included CO₂ treatment and inoculation treatment as categorical fixed effects and nitrogen fertilization as a continuous fixed effect, with all possible interaction terms between all three fixed effects included. Models accounted for climatic differences between chambers across experiment iterations by including a random intercept term that nested the starting chamber rack within CO₂ treatment. Models with this independent variable structure were created for each of the following dependent variables: N_{area} , M_{area} , N_{mass} , Chl_{area} , $A_{net,420}$, $A_{net,gc}$, V_{cmax25} , J_{max25} , $J_{max25}:V_{cmax25}$, R_{d25} , $PNUE_{gc}$, total leaf area, total biomass, total leaf biomass, stem biomass, root biomass, root nodule biomass, root:shoot ratio, leaf mass fraction, stem mass fraction, root mass fraction, below-ground biomass carbon costs to acquire nitrogen, below-ground biomass carbon, whole-plant nitrogen biomass, and the root nodule biomass:root biomass ratio.

Shapiro-Wilk tests of normality were used to assess whether linear mixed-effects models satisfied residual normality assumptions. Models for N_{area} , N_{mass} , Chl_{area} , $A_{net,420}$, $A_{net,gc}$, V_{cmax25} , J_{max25} , $J_{max25}:V_{cmax25}$, R_{d25} , $PNUE_{gc}$, total leaf area, leaf mass fraction, stem mass fraction, below-ground biomass carbon, and whole-plant nitrogen biomass satisfied residual normality assumptions without data transformation. Models for M_{area} , root:shoot ratio, below-ground biomass carbon costs to acquire nitrogen, and root mass fraction satisfied residual normality assumptions with a natural log data transformation. Models for total biomass, leaf biomass, stem biomass, root biomass, root nodule biomass, and root nodule biomass:root biomass satisfied residual normality assumptions with a square root data transformation.

In all models, the 'lmer' function in the 'lme4' R package (Bates *et al.*, 2015) was used to fit each model, and the 'Anova' function in the 'car' R package (Fox and Weisberg, 2019) was used to calculate Type II Wald's χ^2 and determine the significance ($\alpha=0.05$) of each fixed effect coefficient. The 'emmeans' R package (Lenth, 2019) was used to conduct post-hoc comparisons using Tukey's tests, where degrees of freedom were approximated using the Kenward-Roger approach (Kenward and Roger, 1997). Trendlines and error ribbons representing the 95% confidence intervals were drawn in all figures using 'emmeans' outputs across the range in nitrogen fertilization values with a maximum of 36 data points per trendline (Supplementary Table S4). All analyses and plots were conducted in R version 4.1.0 (R Core Team, 2021). Results for N_{mass} and M_{area} (Supplementary Table S5; Supplementary Fig. S1), dark respiration (Supplementary Table S6), and organ biomasses (Supplementary Table S7) are summarized in Supplementary Protocol S1.

Results

Leaf nitrogen content

Elevated CO₂ reduced N_{area} and Chl_{area} by 29% and 30%, respectively ($P<0.001$ in both cases; Table 1; Fig. 1). Increasing nitrogen fertilization increased N_{area} ($P<0.001$; Table 1; Fig. 1) more strongly under ambient CO₂ than elevated CO₂ (CO₂×nitrogen fertilization interaction: $P<0.05$; Table 1), resulting in a stronger reduction in N_{area} under elevated CO₂ as nitrogen fertilization increased (Supplementary Fig. S2). Uninoculated plants experienced a stronger reduction in N_{area} under elevated CO₂ than inoculated plants (CO₂×inoculation interaction: $P<0.05$; Table 1). Increasing nitrogen fertilization increased N_{area} and Chl_{area} ($P<0.001$ in both cases; Table 1; Fig. 1) more strongly in uninoculated plants than in inoculated plants

(inoculation×nitrogen fertilization interaction: $P < 0.001$ in both cases; Table 1).

Gas exchange

Elevated CO₂ decreased $A_{\text{net},420}$ by 17% and increased $A_{\text{net},\text{gc}}$ by 33% ($P < 0.001$ in both cases; Table 2). Increasing nitrogen fertilization increased $A_{\text{net},420}$ and $A_{\text{net},\text{gc}}$ similarly between CO₂ treatments (CO₂×nitrogen fertilization interaction: $P > 0.05$; Table 2; Fig. 2A). Inoculated plants experienced a stronger increase in $A_{\text{net},\text{gc}}$ under elevated CO₂ than uninoculated plants (CO₂×inoculation interaction: $P < 0.05$; Table 2). Increasing nitrogen fertilization increased $A_{\text{net},420}$ and $A_{\text{net},\text{gc}}$ ($P < 0.001$ in both cases; Table 2) more strongly in uninoculated plants than in inoculated plants (inoculation×nitrogen fertilization interaction: $P < 0.001$ in both cases; Fig. 2A, B).

Table 1. Effects of CO₂ concentration, inoculation, and nitrogen fertilization on area-based leaf nitrogen content and chlorophyll content^a

	df	N_{area}		Chl_{area}	
		χ^2	P	χ^2	P
CO ₂	1	155.908	<0.001	62.056	<0.001
Inoculation (I)	1	86.029	<0.001	133.828	<0.001
N fertilization (N)	1	316.408	<0.001	156.659	<0.001
CO ₂ ×I	1	4.729	0.030	1.647	0.199
CO ₂ ×N	1	5.723	0.017	2.780	0.095
I×N	1	43.381	<0.001	73.494	<0.001
CO ₂ ×I×N	1	0.489	0.484	2.123	0.145

^a Significance determined using Type II Wald χ^2 tests ($\alpha = 0.05$). P -values < 0.05 are in bold. df, degrees of freedom; N_{area} , leaf nitrogen content per unit leaf area (gN m^{-2}); Chl_{area} , chlorophyll content per unit leaf area (mmol m^{-2}).

Elevated CO₂ decreased $V_{\text{cmax}25}$ by 16% and $J_{\text{max}25}$ by 10%, increasing $J_{\text{max}25}:V_{\text{cmax}25}$ by 8% ($P < 0.05$ in all cases; Table 2). Increasing nitrogen fertilization increased $V_{\text{cmax}25}$ and $J_{\text{max}25}$, but decreased $J_{\text{max}25}:V_{\text{cmax}25}$, similarly between CO₂ (CO₂×nitrogen fertilization interaction: $P > 0.05$ in all cases; Table 2; Fig. 2B–D) and inoculation treatments (CO₂×inoculation interaction: $P > 0.05$ in all cases; Table 2). Increasing nitrogen fertilization increased $V_{\text{cmax}25}$ and $J_{\text{max}25}$, and decreased $J_{\text{max}25}:V_{\text{cmax}25}$ ($P < 0.001$; Table 2), but these patterns were only observed in uninoculated plants (inoculation×nitrogen fertilization interaction: $P < 0.05$ in all cases).

Photosynthetic nitrogen-use efficiency

Elevated CO₂ increased PNUE_{gc} by 97% ($P < 0.001$; Supplementary Table S6; Supplementary Fig. S3) due to a 33% increase in $A_{\text{net},\text{gc}}$ (Fig. 2A) and a 29% decrease in N_{area} (Fig. 1B). Increasing nitrogen fertilization decreased PNUE_{gc} ($P < 0.001$; Supplementary Table S6) more strongly under elevated CO₂ (CO₂×nitrogen fertilization interaction: $P < 0.05$; Supplementary Table S6; Supplementary Fig. S3), leading to a weaker increase in PNUE_{gc} due to elevated CO₂ as nitrogen fertilization increased (Supplementary Fig. S4). Increasing nitrogen fertilization decreased PNUE_{gc} ($P < 0.001$; Supplementary Table S4), but this pattern was only observed in inoculated plants (inoculation×nitrogen fertilization interaction: $P < 0.05$; Supplementary Table S6; Supplementary Fig. S3).

Total leaf area and total biomass

Elevated CO₂ increased total leaf area and total biomass by 51% and 102%, respectively ($P < 0.001$ in both cases; Table 3). Increasing nitrogen fertilization increased total leaf area and total biomass ($P < 0.001$ in both cases; Table

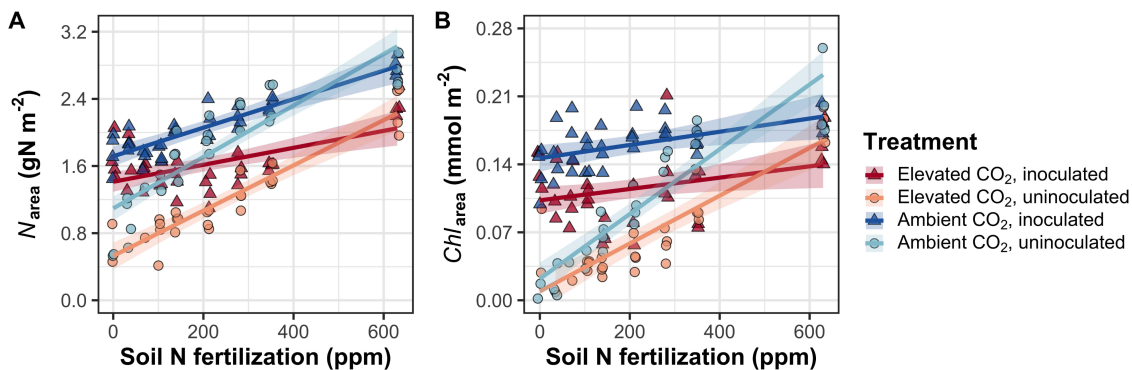


Fig. 1. Effects of CO₂ concentration, inoculation, and nitrogen fertilization on leaf nutrient content. The effects of CO₂ concentration, inoculation, and nitrogen fertilization on leaf nitrogen per unit leaf area (A) and chlorophyll content per unit leaf area (B) are shown. Nitrogen fertilization is on the x-axis in both panels. Red shaded points and trendlines indicate plants grown under elevated CO₂, while blue shaded points and trendlines indicate plants grown under ambient CO₂. Light blue and light red circular points and trendlines indicate measurements collected from uninoculated plants, while dark blue and dark red triangular points indicate measurements collected from inoculated plants. Solid trendlines indicate regression slopes that are different from zero ($P < 0.05$), while dashed trendlines indicate slopes that are not distinguishable from zero ($P > 0.05$). Error ribbons of each trendline represent the upper and lower 95% confidence intervals.

Table 2. Effects of CO₂ concentration, inoculation, and nitrogen fertilization on leaf gas exchange^a

	df	$A_{\text{net},420}$		$A_{\text{net},\text{gc}}$		$V_{\text{cmax}25}$		$J_{\text{max}25}$		$J_{\text{max}25}:V_{\text{cmax}25}$	
		χ^2	<i>P</i>	χ^2	<i>P</i>	χ^2	<i>P</i>	χ^2	<i>P</i>	χ^2	<i>P</i>
CO ₂	1	15.747	<0.001	52.716	<0.001	18.039	<0.001	6.042	0.014	92.010	<0.001
Inoculation (I)	1	77.137	<0.001	83.008	<0.001	98.579	<0.001	85.064	<0.001	27.768	<0.001
N fertilization (N)	1	11.986	<0.001	14.658	<0.001	37.053	<0.001	25.356	<0.001	28.147	<0.001
CO ₂ ×I	1	1.032	0.310	5.634	0.018	0.065	0.799	0.667	0.414	2.916	0.088
CO ₂ ×N	1	1.998	0.158	0.135	0.713	1.758	0.185	0.742	0.389	3.210	0.073
I×N	1	46.800	<0.001	50.774	<0.001	60.394	<0.001	57.41	<0.001	9.607	0.002
CO ₂ ×I×N	1	0.002	0.964	1.332	0.248	0.748	0.387	0.377	0.539	1.102	0.294

^aSignificance determined using Type II Wald χ^2 tests ($\alpha=0.05$). *P*-values <0.05 are in bold. df, degrees of freedom; $A_{\text{net},420}$, net photosynthesis rate at 420 $\mu\text{mol mol}^{-1}$ CO₂ ($\mu\text{mol m}^{-2} \text{s}^{-1}$); $A_{\text{net},\text{gc}}$, net photosynthesis rate under growth CO₂ condition ($\mu\text{mol m}^{-2} \text{s}^{-1}$); $V_{\text{cmax}25}$, apparent maximum rate of Rubisco carboxylation at 25 °C ($\mu\text{mol m}^{-2} \text{s}^{-1}$); $J_{\text{max}25}$, apparent maximum rate of electron transport for RuBP regeneration at 25 °C ($\mu\text{mol m}^{-2} \text{s}^{-1}$).

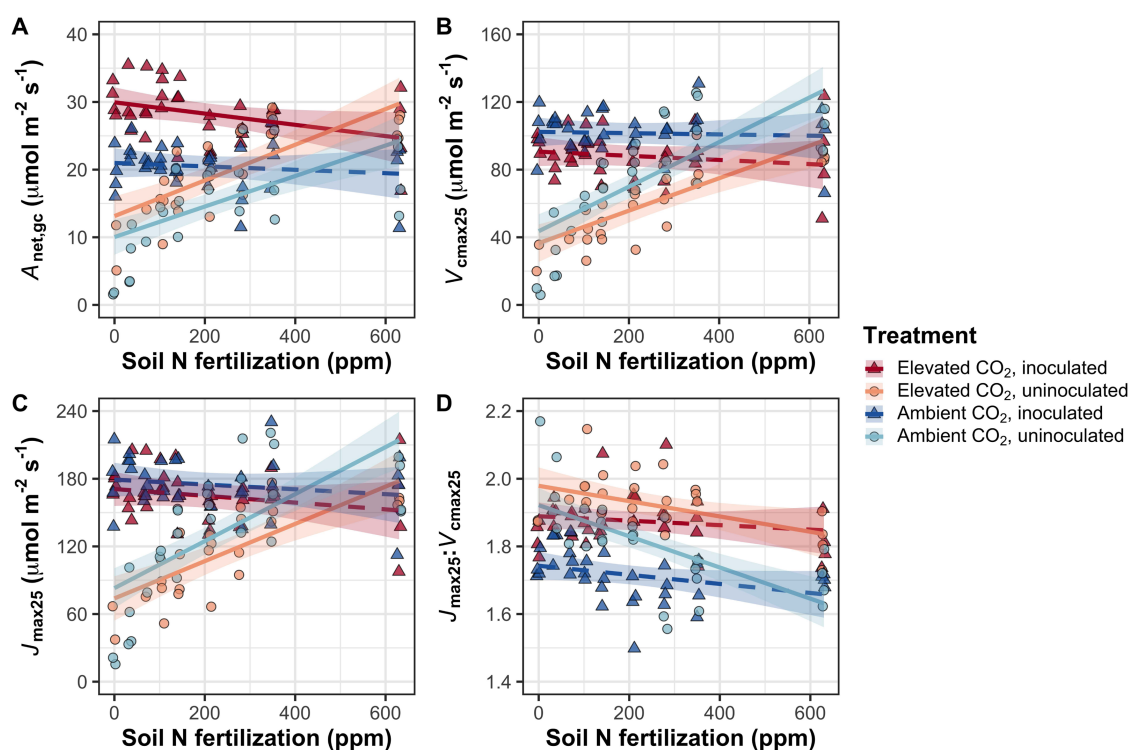


Fig. 2. Effects of CO₂ concentration, inoculation, and nitrogen fertilization on leaf photosynthetic traits. The effects on net photosynthesis measured under growth CO₂ concentration (A), the apparent maximum rate of Rubisco carboxylation at 25 °C (B), the apparent maximum rate of electron transport for RuBP regeneration at 25 °C (C), and the ratio of the apparent maximum rate of electron transport for RuBP regeneration to the apparent maximum rate of Rubisco carboxylation (D) are shown. Nitrogen fertilization is on the x-axis in all panels. Red shaded points and trendlines indicate plants grown under elevated CO₂, while blue shaded points and trendlines indicate plants grown under ambient CO₂. Light blue and light red circular points and trendlines indicate measurements collected from uninoculated plants, while dark blue and dark red triangular points indicate measurements collected from inoculated plants. Solid trendlines indicate regression slopes that are different from zero ($P<0.05$), while dashed trendlines indicate slopes that are not distinguishable from zero ($P>0.05$). Error ribbons of each trendline represent the upper and lower 95% confidence intervals.

3) more strongly under elevated CO₂ than ambient CO₂ (CO₂×nitrogen fertilization interaction: $P<0.001$ in both cases; Table 3), leading to an amplified positive effect of elevated CO₂ on total leaf area and total biomass as nitrogen fertilization increased (Fig. 3A, B). Inoculation had no effect on total leaf area or total biomass responses to elevated CO₂

(CO₂×inoculation interaction: $P>0.05$ in both cases; Table 3). Increasing nitrogen fertilization increased total leaf area and total biomass ($P<0.001$ in both cases; Table 3) more strongly in uninoculated plants than in inoculated plants (inoculation×nitrogen fertilization interaction: $P<0.001$; Table 3; Fig. 3A, B).

Table 3. Effects of CO₂ concentration, inoculation, and nitrogen fertilization on total leaf area, total biomass, carbon costs to acquire nitrogen, and plant investment toward symbiotic nitrogen fixation^a

	df	Total leaf area		Total biomass ^b		Root:shoot ratio ^c	
		χ^2	<i>P</i>	χ^2	<i>P</i>	χ^2	<i>P</i>
CO ₂	1	69.291	<0.001	131.477	<0.001	4.892	0.027
Inoculation (I)	1	35.715	<0.001	34.264	<0.001	9.790	0.002
N fertilization (N)	1	274.199	<0.001	269.046	<0.001	50.742	<0.001
CO ₂ ×I	1	2.064	0.151	0.518	0.472	10.467	0.001
CO ₂ ×N	1	18.655	<0.001	16.877	<0.001	0.012	0.914
I×N	1	10.804	0.001	15.779	<0.001	3.802	0.051
CO ₂ ×I×N	1	<0.001	0.990	0.023	0.880	0.417	0.519

	Carbon cost to acquire nitrogen ^b		Nodule biomass:root biomass	
	χ^2	<i>P</i>	χ^2	<i>P</i>
CO ₂	76.462	<0.001	0.010	0.921
Inoculation (I)	70.846	<0.001	902.063	<0.001
N fertilization (N)	74.961	<0.001	254.741	<0.001
CO ₂ ×I	33.329	<0.001	21.632	<0.001
CO ₂ ×N	1.889	0.169	1.590	0.207
I×N	26.719	<0.001	132.463	<0.001
CO ₂ ×I×N	6.860	0.009	2.481	0.115

^a Significance determined using Type II Wald χ^2 tests ($\alpha=0.05$). *P*-values <0.05 are in bold and *P*-values where $0.05 < P < 0.1$ are in italics. df, degrees of freedom; total leaf area (cm²); total biomass (g); the ratio of root biomass to shoot biomass (unitless), below-ground biomass carbon cost to acquire nitrogen (gC gN⁻¹), the ratio of root nodule biomass to root biomass (unitless).

^b Variable was natural log transformed before model fitting, ^c variable was square root transformed before model fitting.

Biomass partitioning

The root:shoot ratio decreased under elevated CO₂ ($P < 0.05$; Table 3; Fig. 3C), although this pattern was only observed in inoculated plants (CO₂×inoculation interaction: $P < 0.05$; Table 3; Fig. 3C). Reductions in the root:shoot ratio under elevated CO₂ were driven by an increase in the leaf mass fraction under elevated CO₂ ($P < 0.001$; Supplementary Table S7) that was only observed in inoculated plants (CO₂×inoculation interaction: $P < 0.05$; Supplementary Table S7). CO₂ treatment did not affect stem mass fraction ($P > 0.05$; Supplementary Table S7), although an interaction between CO₂ and inoculation treatment indicated that elevated CO₂ increased the root mass fraction in inoculated plants (CO₂×inoculation interaction: $P < 0.05$; Supplementary Table S7). Increasing nitrogen fertilization decreased the root:shoot ratio ($P < 0.001$; Supplementary Table 3), a pattern that was marginally stronger in uninoculated plants than in inoculated plants (CO₂×inoculation interaction: $P = 0.051$; Table 3; Fig. 3C). Increasing nitrogen fertilization increased the leaf mass fraction and decreased the root mass fraction ($P < 0.001$ in both cases; Supplementary Table S7), but these patterns only occurred in uninoculated plants (inoculation×nitrogen fertilization interaction: $P < 0.05$ in both cases; Supplementary Table S7). Increasing nitrogen fertilization increased stem mass fraction ($P < 0.001$; Supplementary Table S7), but these patterns only occurred

in inoculated plants (inoculation×nitrogen fertilization interaction: $P < 0.001$; Supplementary Table S7).

Below-ground biomass carbon cost to acquire nitrogen

Elevated CO₂ increased below-ground biomass carbon costs to acquire nitrogen ($P < 0.001$; Table 3) more strongly in uninoculated plants than in inoculated plants (CO₂×inoculation interaction: $P < 0.001$; Table 3). Increasing nitrogen fertilization decreased carbon costs to acquire nitrogen ($P < 0.001$; Table 3) more strongly in uninoculated plants than in inoculated plants (inoculation×nitrogen fertilization: $P < 0.001$; Table 3; Fig. 3D). Interactions between inoculation and nitrogen fertilization treatments were more pronounced when plants were grown under elevated CO₂ (CO₂×inoculation×nitrogen fertilization interaction: $P < 0.05$; Fig. 3D). This pattern was driven by a strong negative effect of increasing nitrogen fertilization on carbon costs to acquire nitrogen in uninoculated plants grown under elevated CO₂ (Tukey: $P < 0.001$) coupled with no nitrogen fertilization effect in inoculated plants grown under elevated CO₂ (Tukey: $P < 0.001$). Under ambient CO₂, increasing nitrogen fertilization decreased carbon costs to acquire nitrogen similarly between inoculation treatments (Tukey: $P > 0.05$).

Elevated CO₂ increased below-ground biomass carbon by 93% and increased whole-plant nitrogen biomass by 26% ($P < 0.001$ in both cases; Supplementary Table S8). Increasing

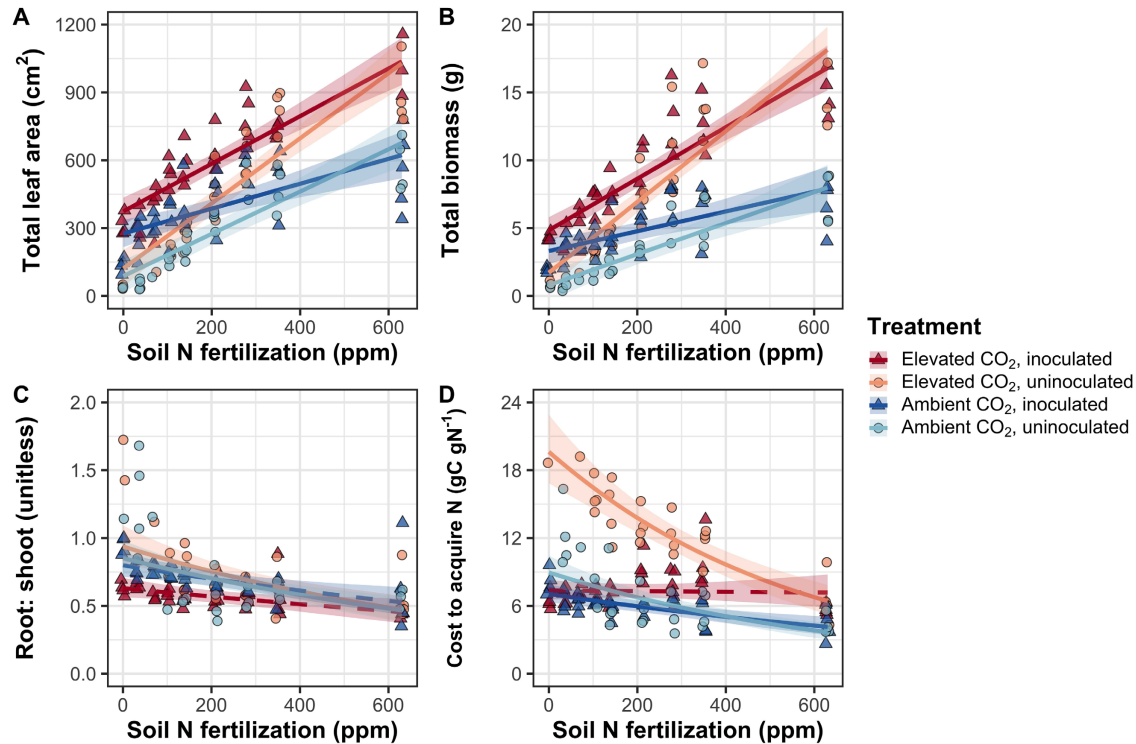


Fig. 3. Effects of CO₂ concentration, inoculation, and nitrogen fertilization on whole-plant traits. Effects on total leaf area (A), total biomass (B), the ratio of root biomass to shoot biomass (C), and below-ground carbon cost to acquire nitrogen (D) are shown. Nitrogen fertilization is on the x-axis in all panels. Red shaded points and trendlines indicate plants grown under elevated CO₂, while blue shaded points and trendlines indicate plants grown under ambient CO₂. Light blue and light red circular points and trendlines indicate measurements collected from uninoculated plants, while dark blue and dark red triangular points indicate measurements collected from inoculated plants. Solid trendlines indicate regression slopes that are different from zero ($P < 0.05$), while dashed trendlines indicate slopes that are not distinguishable from zero ($P > 0.05$). Error ribbons of each trendline represent the upper and lower 95% confidence intervals.

nitrogen fertilization increased below-ground biomass carbon and whole-plant nitrogen biomass more strongly under elevated CO₂ than under ambient CO₂ (CO₂ × nitrogen fertilization interaction: $P < 0.001$; [Supplementary Table S8](#); [Supplementary Fig. S5](#)). These patterns resulted in an amplified positive effect of elevated CO₂ on below-ground biomass carbon and whole-plant nitrogen biomass as nitrogen fertilization increased, though this pattern was stronger for whole-plant nitrogen biomass than below-ground biomass carbon ([Supplementary Fig. S5](#)). Increasing nitrogen fertilization increased below-ground biomass carbon and whole-plant nitrogen biomass ($P < 0.001$; [Supplementary Table S8](#)) more strongly in uninoculated plants than in inoculated plants (inoculation × nitrogen fertilization interaction: $P < 0.001$ in both cases; [Supplementary Table S8](#); [Supplementary Fig. S5](#)).

Plant investment toward symbiotic nitrogen fixation

CO₂ treatment did not affect root nodule:root biomass ($P > 0.05$; [Table 3](#); [Fig. 4](#)) despite anecdotally stronger positive effects of elevated CO₂ on root biomass (96% increase; $P < 0.001$; [Supplementary Table S7](#)) than on root nodule

biomass (70% increase; $P < 0.001$; [Supplementary Table S7](#)). Increasing nitrogen fertilization decreased root nodule:root biomass ($P < 0.001$; [Table 3](#)) more strongly in inoculated plants than in uninoculated plants (inoculation × nitrogen fertilization interaction: $P < 0.001$; [Table 3](#); [Fig. 4](#)).

Discussion

Glycine max plants were grown under two CO₂ concentrations, two inoculation treatments, and nine nitrogen fertilization treatments in a full-factorial growth chamber experiment. We used data collected from this experiment to (i) determine whether plant responses to elevated CO₂ aligned more closely with the nitrogen limitation or eco-evolutionary optimality hypothesis and (ii) assess how the ability to associate with symbiotic nitrogen-fixing bacteria might influence these responses.

Leaf photosynthetic responses to elevated CO₂ are unrelated to nitrogen availability

Individuals grown under elevated CO₂ experienced a reduction in $A_{\text{net},420}$ ([Table 2](#)), leaf nitrogen content ([Fig. 1A](#),

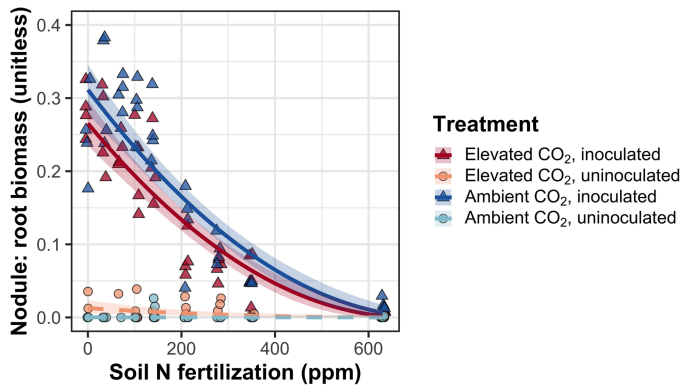


Fig. 4. Effects of CO₂ concentration, inoculation, and nitrogen fertilization on the ratio of root nodule biomass to root biomass. Nitrogen fertilization is on the x-axis. Red shaded points and trendlines indicate plants grown under elevated CO₂, while blue shaded points and trendlines indicate plants grown under ambient CO₂. Light blue and light red circular points and trendlines indicate measurements collected from uninoculated plants, while dark blue and dark red triangular points indicate measurements collected from inoculated plants. Solid trendlines indicate regression slopes that are different from zero ($P < 0.05$), while dashed trendlines indicate slopes that are not distinguishable from zero ($P > 0.05$). Error ribbons of each trendline represent the upper and lower 95% confidence intervals.

Supplementary Fig. S1), $V_{\text{cmax}25}$ (Fig. 2B), and $J_{\text{max}25}$ (Fig. 2C) compared with plants grown under ambient CO₂. These patterns suggest a down-regulation of leaf-level investment toward photosynthetic enzymes under elevated CO₂. This down-regulation was probably driven by increased Rubisco affinity for carboxylation relative to oxygenation, which decreased leaf-level demand to build and maintain photosynthetic enzymes (Bazzaz, 1990; Dong *et al.*, 2022). Despite reduced investment toward photosynthetic enzymes, elevated CO₂ increased $A_{\text{net,gc}}$ (Fig. 2A). This response was associated with a reduction in N_{area} and a larger reduction in $V_{\text{cmax}25}$ than $J_{\text{max}25}$, which increased PNUE (Supplementary Fig. S3B) and $J_{\text{max}25}:V_{\text{cmax}25}$, and allowed enhanced $A_{\text{net,gc}}$ to be achieved by approaching optimal coordination (Chen *et al.*, 1993; Maire *et al.*, 2012; Smith and Keenan, 2020). These patterns are consistent with our expectations and previous studies that have investigated leaf photosynthetic responses to elevated CO₂ (Drake *et al.*, 1997; Ainsworth *et al.*, 2002; Ainsworth and Long, 2005; Ainsworth and Rogers, 2007; Crous *et al.*, 2010; Lee *et al.*, 2011; Smith and Dukes, 2013; Poorter *et al.*, 2022; Cui *et al.*, 2023; Stocker *et al.*, 2025).

Positive effects of elevated CO₂ on $A_{\text{net,gc}}$ (Fig. 2A) and $J_{\text{max}25}:V_{\text{cmax}25}$ (Fig. 2D), and negative effects of elevated CO₂ on $A_{\text{net,420}}$, $V_{\text{cmax}25}$, and $J_{\text{max}25}$ (Fig. 2A–C) were not modified by nitrogen fertilization, as the slope that explained the effects of increasing nitrogen fertilization on each of these traits was similar between CO₂ treatments. Instead, the increase in $J_{\text{max}25}:V_{\text{cmax}25}$ (Fig. 2D) and PNUE_{gc} (Supplementary Fig. S3B) under elevated CO₂ provides strong support for the idea that leaves were down-regulating $V_{\text{cmax}25}$ in response to elevated CO₂ such that enhanced $A_{\text{net,gc}}$ could be achieved by

approaching optimal coordination of Rubisco carboxylation and electron transport for RuBP regeneration (Chen *et al.*, 1993; Maire *et al.*, 2012; Smith and Keenan, 2020).

Negative effects of elevated CO₂ on mass- and area-based leaf nitrogen content became more pronounced with increasing nitrogen fertilization (Supplementary Fig. S2A, B). Since nitrogen fertilization did not affect photosynthetic responses to elevated CO₂, this decline in leaf nitrogen content may reflect reduced allocation to non-photosynthetic pools, such as structural tissue or chemical pathways that contribute to herbivore defense (Zavala *et al.*, 2013; Onoda *et al.*, 2017; Johnson *et al.*, 2020). While not a primary focus of this study, understanding leaf nitrogen allocation responses to elevated CO₂ across nitrogen availability gradients would help clarify the role of leaf nitrogen allocation in leaf-level responses to elevated CO₂.

Overall, leaf photosynthetic responses to elevated CO₂ showed strong support for the eco-evolutionary optimality hypothesis. Photosynthetic responses to elevated CO₂ were independent from nitrogen fertilization, suggesting that these responses were wholly determined through changes in leaf-level demand to build and maintain photosynthetic enzymes. These findings also reinforce previous work showing that leaf photosynthetic responses to elevated CO₂ are decoupled from nitrogen availability (Lee *et al.*, 2011; Pastore *et al.*, 2019; Smith and Keenan, 2020; Harrison *et al.*, 2021). Additionally, our results indicate that optimal resource investment in photosynthetic capacity may function as a nitrogen-saving mechanism that allows plants to maximize resource-use efficiency at the leaf level as a strategy for maximizing resource allocation to whole-plant growth (Smith and Keenan, 2020; Smith *et al.*, 2024).

Whole-plant responses to elevated CO₂ are constrained by nitrogen availability

Leaf photosynthetic responses to elevated CO₂ corresponded with increased total leaf area and total biomass (Fig. 3A, B), supporting previous work (Ainsworth *et al.*, 2002; Ainsworth and Long, 2005; Smith and Dukes, 2013; Poorter *et al.*, 2022; Stocker *et al.*, 2025). Increased total leaf area increased whole-plant capacity for light interception, boosting whole-plant photosynthesis and supporting biomass accumulation when coupled with an increase in leaf-level $A_{\text{net,gc}}$. In contrast to expectations and previous work (Nie *et al.*, 2013; Stocker *et al.*, 2025), elevated CO₂ decreased the root-to-shoot ratio (Fig. 3C) through an increase in the leaf mass fraction and no change in the stem or root mass fractions (Supplementary Table S7). Despite this, plants experienced an increase in root biomass (Supplementary Fig. S6) and below-ground carbon allocation (Supplementary Fig. S5) under elevated CO₂, suggesting that plants responded to heightened whole-plant demand under elevated CO₂ by investing in structures that support nutrient acquisition even if they allocated relatively more biomass above-ground.

Increasing nitrogen fertilization enhanced the positive effects of elevated CO₂ on total leaf area and total biomass (Fig. 3A, B). Interestingly, this interaction revealed no effect of CO₂ treatment on total leaf area in uninoculated individuals under low nitrogen fertilization, supporting previous work showing that CO₂ fertilization effects on traits related to whole-plant growth are often absent under low nutrient availability (Sigurdsson *et al.*, 2013). Similar effects of CO₂ treatment on total leaf area under low nitrogen fertilization may have been due to plants being unable to satisfy demand for soil nitrogen similarly between the two CO₂ treatments. Stronger positive effects of elevated CO₂ on total leaf area and total biomass with increasing nitrogen fertilization were associated with stronger increases in below-ground carbon allocation and whole-plant nitrogen uptake (Supplementary Fig. S5), supporting the nitrogen limitation hypothesis (Luo *et al.*, 2004; Reich *et al.*, 2006; Norby *et al.*, 2010; Feng *et al.*, 2015). These findings indicate that plants grown under elevated CO₂ satisfied the greater whole-plant demand to build new tissues by increasing investment in nitrogen acquisition. Despite this, nitrogen fertilization did not modify whether plants invested in above-ground or below-ground tissues in response to elevated CO₂, as indicated by similar positive effects of increasing nitrogen fertilization on the root-to-shoot ratio (Fig. 3C) and all organ mass fractions between CO₂ treatments (Supplementary Table S7). These responses indicate that biomass allocation responses to elevated CO₂ were more strongly dictated by changes in whole-plant demand to build new tissues than the supply of nutrients, even though overall biomass responses to elevated CO₂ were regulated by nitrogen availability.

Inoculation does not affect leaf or whole-plant responses to elevated CO₂

Inoculation increased N_{area} (Fig. 1A), $A_{\text{net},420}$, $A_{\text{net},\text{gc}}$ (Fig. 2A), $V_{\text{cmax}25}$ (Fig. 2B), $J_{\text{max}25}$ (Fig. 2C), total leaf area (Fig. 3A), and total biomass (Fig. 3B), but decreased $J_{\text{max}25}:V_{\text{cmax}25}$ (Fig. 2D). These results support previous studies suggesting that species forming symbiotic associations with nitrogen-fixing bacteria have greater leaf nitrogen content, photosynthetic capacity, and growth than those that do not (Adams *et al.*, 2016; Bytnerowicz *et al.*, 2023). The positive effects of inoculation on leaf and whole-plant traits were strongest under low nitrogen fertilization and diminished with increasing nitrogen fertilization due to a reduction in plant investment toward symbiotic nitrogen fixation as nitrogen fertilization increased (Fig. 4). These patterns support the idea that forming associations with symbiotic nitrogen-fixing bacteria confers a competitive advantage in nitrogen-limited environments, where access to a less finite nitrogen pool (i.e. the atmosphere) allows plants to satisfy demand more efficiently than relying on limited soil nitrogen (Rastetter *et al.*, 2001; Andrews *et al.*, 2011; McCulloch and Porder, 2021).

Inoculation had no effect on leaf or whole-plant responses to elevated CO₂, but played a strong role in determining the effect of nitrogen fertilization on measured traits. The null inoculation effect on plant responses to elevated CO₂ was consistent across the nitrogen fertilization gradient, contrary to our hypothesis that inoculation would enhance plant responses to elevated CO₂ most strongly under low nitrogen fertilization (Rastetter *et al.*, 2001; Perkowski *et al.*, 2021). Previous research has highlighted that nitrogen-fixing species typically show stronger responses to elevated CO₂ than non-fixing species (Ainsworth *et al.*, 2002; Ainsworth and Long, 2005), although some studies question the generality of this pattern (Nowak *et al.*, 2004; Rogers *et al.*, 2009). Our findings assert that the ability to associate with symbiotic nitrogen-fixing bacteria played no role in determining whether plant responses to elevated CO₂ aligned with the nitrogen limitation or eco-evolutionary optimality hypothesis, even though inoculated individuals grown under elevated CO₂ exhibited greater root nodule biomass (Supplementary Fig. S6A) and reduced carbon costs to acquire nitrogen (Fig. 3D) compared with those grown under ambient CO₂.

As mentioned, plants grown under elevated CO₂ exhibited greater root nodule biomass (Supplementary Fig. S6A). This pattern indicates that plants responded to heightened whole-plant demand for new tissue growth by increasing nitrogen uptake through nitrogen fixation. However, the increase in root nodule biomass was circumvented by a stronger increase in root biomass (Supplementary Fig. S6B). This pattern indicates an investment shift toward direct uptake with increasing CO₂, a response that contrasts with previous work showing that plants increase investment in microbial symbionts when whole-plant demand to build new tissues increases (Taylor and Menge, 2018; Friel and Friesen, 2019; Perkowski *et al.*, 2021). Increased relative allocation to root biomass may have been a strategy to prioritize the acquisition of non-nitrogen resources, as nitrogen fixation may increase the extent by which physiology and plant growth become limited by other nutrients, such as phosphorus (Finzi and Rodgers, 2009). Previous research has shown that phosphorus plays a key role in shaping plant responses to elevated CO₂ and that the benefits of nitrogen fixation under elevated CO₂ become more apparent when other nutrients (e.g. phosphorus) are available in sufficient supply (van Groenigen *et al.*, 2006; Jiang *et al.*, 2020). Thus, null effects of inoculation on plant responses to elevated CO₂ may have been driven by phosphorus co-limitation, although future work is needed to test this hypothesis.

Modeling implications

Many terrestrial biosphere models predict photosynthetic capacity through parameterized relationships between N_{area} and V_{cmax} (Smith and Dukes, 2013; Rogers *et al.*, 2017), which assumes that leaf nitrogen-photosynthesis relationships are constant across growing environments. Our results build on

previous work suggesting that leaf nitrogen–photosynthesis relationships dynamically change across growing environments (Luo *et al.*, 2021; Waring *et al.*, 2023). Specifically, elevated CO₂ reduced leaf nitrogen content (Fig. 1A) more strongly than it increased $A_{\text{net,gc}}$ (Fig. 2A) and decreased $V_{\text{cmax}25}$ (Fig. 2B) and $J_{\text{max}25}$ (Fig. 2C), while inoculation increased $V_{\text{cmax}25}$ and $J_{\text{max}25}$ more strongly than it increased leaf nitrogen content. These patterns indicate that elevated CO₂ increased the fractional pool of leaf nitrogen content allocated to Rubisco and bioenergetics, while inoculation decreased the fraction of leaf nitrogen content allocated to these pools (Niinemets and Tenhunen, 1997).

Increasing nitrogen fertilization increased indices of apparent photosynthetic capacity, but this pattern was only observed in uninoculated plants. Increasing nitrogen fertilization also increased N_{area} and Chl_{area} more strongly in uninoculated plants (Fig. 1). Eco-evolutionary optimality theory predicts that plants should exhibit strong positive effects of increasing nitrogen availability on photosynthetic traits when nitrogen availability is insufficient for satisfying leaf-level demand for photosynthesis, or when changes in nitrogen availability decrease the relative costs of nitrogen acquisition and use compared with those of water acquisition and use (Wright *et al.*, 2003; Harrison *et al.*, 2021; Stocker *et al.*, 2025). In cases where nitrogen availability exceeds leaf-level demand for photosynthesis or costs to acquire nitrogen relative to water increase, the theory predicts that positive effects of increasing nitrogen availability on photosynthesis should diminish, with excess nitrogen not needed to satisfy leaf-level demand for photosynthesis being allocated toward the construction of other plant tissues (e.g. additional leaves). Given this, strong positive effects of increasing nitrogen fertilization on indices of photosynthetic capacity in uninoculated plants were expected, as uninoculated plants were nitrogen limited under low nitrogen fertilization and could not meet the leaf-level demand for photosynthetic enzymes. We found some evidence for a diminished positive effect of nitrogen fertilization on photosynthetic traits, with uninoculated plants demonstrating smaller increases in $V_{\text{cmax}25}$ between 350 ppm N and 630 ppm N (39% increase) than between 0 ppm N and 280 ppm N (79% increase). In contrast, nitrogen fertilization effects on photosynthetic traits were absent in inoculated individuals. This pattern was also expected, as inoculated plants were able to acquire sufficient nitrogen across the nitrogen availability gradient to satisfy leaf-level photosynthetic demand, investing more strongly in microbial symbionts under low nitrogen fertilization and shifting to nitrogen acquisition through direct uptake pathways as nitrogen became more available.

Overall, these results indicate that leaf nitrogen–photosynthesis relationships are context dependent on nitrogen acquisition strategy, may only be constant in environments where nitrogen availability limits leaf physiology, and will probably shift in response to increasing atmospheric CO₂ concentrations. Terrestrial biosphere models that predict photosynthetic

capacity through parameterized relationships between N_{area} and V_{cmax} (Kattge *et al.*, 2009; Walker *et al.*, 2014) may risk overestimating photosynthetic capacity, therefore net primary productivity and the magnitude of the land carbon sink, under future novel growth environments.

Our results demonstrate that optimal resource allocation to photosynthetic capacity defines leaf photosynthetic responses to elevated CO₂ and that these responses are not modified by nitrogen availability. Current approaches for simulating photosynthetic responses to CO₂ in terrestrial biosphere models with coupled carbon and nitrogen cycles often invoke patterns expected from the nitrogen limitation hypothesis, where nitrogen availability diminishes with time due to increasing CO₂ concentrations because whole-plant nitrogen demand continually exceeds supply, depleting the pool of nitrogen available for plants to acquire and allocate to the construction and maintenance of new tissues. This response causes models to simulate a reduction in leaf nitrogen content and therefore photosynthetic capacity, as leaf-level photosynthesis is commonly modeled as a function of positive relationships between nitrogen availability, leaf nitrogen content, and photosynthetic capacity (Smith and Dukes, 2013; Rogers *et al.*, 2017). Findings presented here contradict this framework, suggesting that leaf photosynthetic responses to elevated CO₂ result in optimized nitrogen allocation to satisfy reduced leaf nitrogen demand to build and maintain photosynthetic enzymes. Optimality models that use principles from eco-evolutionary optimality theory can capture photosynthetic responses to CO₂ independent of nitrogen availability (Smith and Keenan, 2020; Harrison *et al.*, 2021; Stocker *et al.*, 2025), suggesting that the inclusion of such frameworks may improve the accuracy with which terrestrial biosphere models simulate photosynthetic processes with increasing atmospheric CO₂ concentrations.

Limitations

Previous work highlights that pot experiments restrict below-ground rooting volume and may alter plant allocation responses to environmental change (Ainsworth *et al.*, 2002; Poorter *et al.*, 2012). In this study, the ratio of pot volume to total biomass was greater under elevated CO₂ and increased with increasing nitrogen fertilization such that several treatment combinations exceeded values recommended to avoid growth limitation imposed by pot volume (<1 g l⁻¹; Supplementary Table S9; Supplementary Fig. S7; Poorter *et al.*, 2012). However, there was no evidence to suggest that pot size limited plant growth, as shown by the lack of a saturating effect of increasing fertilization on total biomass, below-ground carbon biomass, or root biomass under conditions where biomass:pot volume ratios exceeded 1 g l⁻¹ (e.g. individuals of either inoculation status grown under high fertilization and elevated CO₂). Field studies that do not restrict below-ground rooting volume have observed similar leaf and whole-plant

responses to elevated CO₂ (Crous *et al.*, 2010; Lee *et al.*, 2011; Pastore *et al.*, 2019; Smith and Keenan, 2020), indicating that the pot volume used in this study (6 liters) was sufficient to avoid growth limitation.

Importantly, there are inherent limitations in using a pot experiment to make inferences about how nitrogen availability modifies community- or ecosystem-level responses to elevated CO₂. While we caution against using this study to make such extrapolations, a similar experiment conducted under field conditions would help validate the patterns observed here while providing insight into how resource competition within and across species may shape plant responses to nitrogen availability and elevated CO₂.

Conclusions

Our study provides strong support for the eco-evolutionary optimality hypothesis at the leaf level, where leaf photosynthetic responses to elevated CO₂ were independent of nitrogen fertilization and inoculation treatment. Instead, elevated CO₂ reduced the maximum rate of Rubisco carboxylation more strongly than it reduced the maximum rate of electron transport for RuBP regeneration, allowing plants to achieve greater net photosynthesis rates under elevated CO₂ by approaching optimal coordination while reducing leaf nitrogen demand to build and maintain photosynthetic enzymes. At the whole-plant level, nitrogen availability played a central role in regulating plant responses to elevated CO₂, consistent with the nitrogen limitation hypothesis. Specifically, increases in total leaf area, total biomass, and plant nitrogen under elevated CO₂ were enhanced with increasing nitrogen fertilization.

While inoculation increased root nodulation under elevated CO₂, it did not significantly enhance whole-plant responses to elevated CO₂, even under low nitrogen conditions where plants were most strongly invested in symbiotic nitrogen-fixing bacteria. This response may have been due to stronger increases in root biomass that caused plants to prioritize direct nitrogen uptake pathways over symbiotic nitrogen fixation as whole-plant demand to build new tissues increased, perhaps as a strategy to reduce co-limitation by other nutrients, such as phosphorus.

Overall, plants grown under elevated CO₂ responded to increased nitrogen availability by increasing the number of optimally coordinated leaves, while changes in nitrogen availability did not modify the down-regulation in apparent photosynthetic capacity under elevated CO₂. The differential role of nitrogen availability on leaf and whole-plant responses to elevated CO₂ and the dynamic leaf nitrogen-photosynthesis relationships across CO₂ and nitrogen fertilization treatments suggest that terrestrial biosphere models may improve simulations of photosynthetic responses to increasing atmospheric CO₂ concentrations by adopting frameworks that include optimality principles.

Supplementary data

The following supplementary data are available at [JXB online](#).

Protocol S1. A continuance of the Results describing the effects of treatment combinations on mass-based leaf nitrogen content and leaf mass per unit leaf area, organ biomass, and the ratio of total biomass to pot volume.

Table S1. Summary table of the volumes of compounds used to create modified Hoagland's solutions for each soil nitrogen fertilization treatment.

Table S2. Summary of the daily growth chamber growing conditions program.

Table S3. Replication scheme for each unique CO₂×inoculation×N fertilization combination.

Table S4. Replication scheme for each unique CO₂×inoculation combination.

Table S5. Effects of treatment combinations on leaf nitrogen content and leaf mass per area.

Table S6. Effects of treatment combinations on dark respiration and photosynthetic nitrogen-use efficiency.

Table S7. Effects of treatment combinations on biomass partitioning.

Table S8. Effects of treatment combinations on components of the carbon cost to acquire nitrogen.

Table S9. Effects of treatment combinations on the ratio of total biomass to pot volume.

Fig. S1. Effects of treatment combinations on mass-based leaf nitrogen content and leaf biomass per unit leaf area.

Fig. S2. Effects of CO₂ and nitrogen fertilization on area-based leaf nitrogen content, mass-based leaf nitrogen content, and leaf biomass per unit leaf area.

Fig. S3. Effects of treatment combinations on dark respiration at 25 °C and photosynthetic nitrogen-use efficiency at growth CO₂ concentration.

Fig. S4. Effects of CO₂ and nitrogen fertilization on photosynthetic nitrogen-use efficiency at growth CO₂ concentration.

Fig. S5. Effects of treatment combinations on below-ground biomass carbon and total nitrogen biomass.

Fig. S6. Effects of treatment combinations on root nodule biomass and root biomass.

Fig. S7. Effects of treatment combinations on the ratio of whole-plant biomass to pot volume.

Acknowledgements

This study is a contribution to the LEMONTREE (Land Ecosystem Models based On New Theory, observations and Experiments) project, receiving support through Schmidt Sciences, LLC. EAP acknowledges support from a Texas Tech University Doctoral Dissertation Completion Fellowship and a Botanical Society of America Graduate Student Research Award. This work was also supported by US National Science Foundation awards to NGS (DEB-2045968 and DEB-2217353).

Author contributions

EAP: conceptualized the study objectives and designed the experiment in collaboration with NGS, collected data, conducted data analysis, and wrote the first manuscript draft; EE: assisted with data collection and experiment maintenance; NGS: conceptualized study objectives and experimental design with EAP, and oversaw experiment progress. All authors provided manuscript feedback and approved the manuscript in its current form.

Conflict of interest

The authors declare no conflicts of interest.

Funding

US National Science Foundation (DEB-2045968 and DEB-2217353), Schmidt Sciences, LLC.

Data availability

All primary data to support the findings of this study are openly available on Zenodo at <https://doi.org/10.5281/zenodo.14962595> (Perkowski *et al.*, 2025).

References

- Adams MA, Turnbull TL, Sprent JI, Buchmann N. 2016. Legumes are different: leaf nitrogen, photosynthesis, and water use efficiency. *Proceedings of the National Academy of Sciences, USA* **113**, 4098–4103.
- Ainsworth EA, Davey PA, Bernacchi CJ, *et al.* 2002. A meta-analysis of elevated [CO₂] effects on soybean (*Glycine max*) physiology, growth and yield. *Global Change Biology* **8**, 695–709.
- Ainsworth EA, Long SP. 2005. What have we learned from 15 years of free-air CO₂ enrichment (FACE)? A meta-analytic review of the responses of photosynthesis, canopy properties and plant production to rising CO₂. *New Phytologist* **165**, 351–371.
- Ainsworth EA, Rogers A. 2007. The response of photosynthesis and stomatal conductance to rising [CO₂]: mechanisms and environmental interactions. *Plant, Cell & Environment* **30**, 258–270.
- Allen K, Fisher JB, Phillips RP, Powers JS, Brzostek ER. 2020. Modeling the carbon cost of plant nitrogen and phosphorus uptake across temperate and tropical forests. *Frontiers in Forests and Global Change* **3**, 43.
- Andrews M, James EK, Sprent JI, Boddey RM, Gross E, dos Reis FB. 2011. Nitrogen fixation in legumes and actinorhizal plants in natural ecosystems: values obtained using ¹⁵N natural abundance. *Plant Ecology and Diversity* **4**, 131–140.
- Arora VK, Katavouta A, Williams RG, *et al.* 2020. Carbon-concentration and carbon-climate feedbacks in CMIP6 models and their comparison to CMIP5 models. *Biogeosciences* **17**, 4173–4222.
- Barber SA. 1962. A diffusion and mass-flow concept of soil nutrient availability. *Soil Science* **93**, 39–49.
- Barnes JD, Balaguer L, Manrique E, Elvira S, Davison AW. 1992. A reappraisal of the use of DMSO for the extraction and determination of chlorophylls a and b in lichens and higher plants. *Environmental and Experimental Botany* **32**, 85–100.
- Bates D, Mächler M, Bolker B, Walker S. 2015. Fitting linear mixed-effects models using lme4. *Journal of Statistical Software* **67**, 1–48.
- Bazzaz FA. 1990. The response of natural ecosystems to the rising global CO₂ levels. *Annual Review of Ecology and Systematics* **21**, 167–196.
- Bernacchi CJ, Morgan PB, Ort DR, Long SP. 2005. The growth of soybean under free air [CO₂] enrichment (FACE) stimulates photosynthesis while decreasing in vivo Rubisco capacity. *Planta* **220**, 434–446.
- Bernacchi CJ, Singsaas EL, Pimentel C, Portis AR, Long SP. 2001. Improved temperature response functions for models of Rubisco-limited photosynthesis. *Plant, Cell & Environment* **24**, 253–259.
- Brzostek ER, Fisher JB, Phillips RP. 2014. Modeling the carbon cost of plant nitrogen acquisition: mycorrhizal trade-offs and multipath resistance uptake improve predictions of retranslocation. *Journal of Geophysical Research, Biogeosciences* **119**, 1684–1697.
- Bytnerowicz TA, Funk JL, Menge DNL, Perakis SS, Wolf AA. 2023. Leaf nitrogen affects photosynthesis and water use efficiency similarly in nitrogen-fixing and non-fixing trees. *Journal of Ecology* **111**, 2457–2471.
- Chen J-L, Reynolds JF, Harley PC, Tenhunen JD. 1993. Coordination theory of leaf nitrogen distribution in a canopy. *Oecologia* **93**, 63–69.
- Cheaib A, Chieppa J, Perkowski EA, Smith NG. 2025. Soil resource acquisition strategy modulates global plant nutrient and water economics. *New Phytologist Early View*. <https://doi.org/10.1111/nph.70087>
- Coleman JS, McConnaughay KDM, Bazzaz FA. 1993. Elevated CO₂ and plant nitrogen-use: is reduced tissue nitrogen concentration size-dependent? *Oecologia* **93**, 195–200.
- Crous KY, Reich PB, Hunter MD, Ellsworth DS. 2010. Maintenance of leaf N controls the photosynthetic CO₂ response of grassland species exposed to 9 years of free-air CO₂ enrichment. *Global Change Biology* **16**, 2076–2088.
- Cui E, Xia J, Luo Y. 2023. Nitrogen use strategy drives interspecific differences in plant photosynthetic CO₂ acclimation. *Global Change Biology* **29**, 3667–3677.
- Curtis PS. 1996. A meta-analysis of leaf gas exchange and nitrogen in trees grown under elevated carbon dioxide. *Plant, Cell & Environment* **19**, 127–137.
- Davies-Barnard T, Meyerholt J, Zaehle S, *et al.* 2020. Nitrogen cycling in CMIP6 land surface models: progress and limitations. *Biogeosciences* **17**, 5129–5148.
- Davies-Barnard T, Zaehle S, Friedlingstein P. 2022. Assessment of the impacts of biological nitrogen fixation structural uncertainty in CMIP6 earth system models. *Biogeosciences* **19**, 3491–3503.
- Dong N, Wright IJ, Chen JM, Luo X, Wang H, Keenan TF, Smith NG, Prentice IC. 2022. Rising CO₂ and warming reduce global canopy demand for nitrogen. *New Phytologist* **235**, 1692–1700.
- Drake BG, González-Meler MA, Long SP. 1997. More efficient plants: a consequence of rising atmospheric CO₂? *Annual Review of Plant Physiology and Plant Molecular Biology* **48**, 609–639.
- Duursma RA. 2015. Plantecophys—an R package for analysing and modelling leaf gas exchange data. *PLoS One* **10**, e0143346.
- Evans JR. 1989. Photosynthesis and nitrogen relationships in leaves of C₃ plants. *Oecologia* **78**, 9–19.
- Evans JR, Clarke VC. 2019. The nitrogen cost of photosynthesis. *Journal of Experimental Botany* **70**, 7–15.
- Farquhar GD, von Caemmerer S, Berry JA. 1980. A biochemical model of photosynthetic CO₂ assimilation in leaves of C₃ species. *Planta* **149**, 78–90.
- Feng Z, Rütting T, Pleijel H, Wallin G, Reich PB, Kammann CI, Newton PCD, Kobayashi K, Luo Y, Uddling J. 2015. Constraints to nitrogen acquisition of terrestrial plants under elevated CO₂. *Global Change Biology* **21**, 3152–3168.
- Field CB, Mooney HA. 1986. Photosynthesis–nitrogen relationship in wild plants. On the economy of plant form and function: *Proceedings of the Sixth Maria Moors Cabot Symposium, Evolutionary Constraints on Primary Productivity, Adaptive Patterns of Energy Capture in Plants*. Harvard Forest, August 1983. Cambridge, UK: Cambridge University Press.
- Finizzi AC, Moore DJP, DeLucia EH, *et al.* 2006. Progressive nitrogen limitation of ecosystem processes under elevated CO₂ in a warm-temperate forest. *Ecology* **87**, 15–25.

- Finzi AC, Norby RJ, Calfapietra C, et al.** 2007. Increases in nitrogen uptake rather than nitrogen-use efficiency support higher rates of temperate forest productivity under elevated CO₂. *Proceedings of the National Academy of Sciences, USA* **104**, 14014–14019.
- Finzi AC, Rodgers VL.** 2009. Bottom-up rather than top-down processes regulate the abundance and activity of nitrogen fixing plants in two Connecticut old-field ecosystems. *Biogeochemistry* **95**, 309–321.
- Fisher JB, Sitch S, Malhi Y, Fisher RA, Huntingford C, Tan S-Y.** 2010. Carbon cost of plant nitrogen acquisition: a mechanistic, globally applicable model of plant nitrogen uptake, retranslocation, and fixation. *Global Biogeochemical Cycles* **24**, 1–17.
- Fox J, Weisberg S.** 2019. *An R companion to applied regression*. Thousand Oaks, CA: Sage.
- Friel CA, Friesen ML.** 2019. Legumes modulate allocation to rhizobial nitrogen fixation in response to factorial light and nitrogen manipulation. *Frontiers in Plant Science* **10**, 1316.
- Gutschick VP.** 1981. Evolved strategies in nitrogen acquisition by plants. *The American Naturalist* **118**, 607–637.
- Harrison SP, Cramer W, Franklin O, et al.** 2021. Eco-evolutionary optimality as a means to improve vegetation and land-surface models. *New Phytologist* **231**, 2125–2141.
- Hoagland DR, Arnon DI.** 1950. The water-culture method for growing plants without soil. California Agricultural Experiment Station Circular No. 347.
- Hungate BA, Dukes JS, Shaw MR, Luo Y, Field CB.** 2003. Nitrogen and climate change. *Science* **302**, 1512–1513.
- IPCC. 2021. *Climate change 2021: the physical science basis*. Contribution of Working Group I to the sixth assessment report of the Intergovernmental Panel on Climate Change. Cambridge, UK and New York, USA: Cambridge University Press.
- Iversen CM.** 2010. Digging deeper: fine-root responses to rising atmospheric CO₂ concentration in forested ecosystems. *New Phytologist* **186**, 346–357.
- Iversen CM, Ledford J, Norby RJ.** 2008. CO₂ enrichment increases carbon and nitrogen input from fine roots in a deciduous forest. *New Phytologist* **179**, 837–847.
- Jiang M, Caldaru S, Zhang H, et al.** 2020. Low phosphorus supply constrains plant responses to elevated CO₂: a meta-analysis. *Global Change Biology* **26**, 5856–5873.
- Johnson SN, Waterman JM, Hall CR.** 2020. Increased insect herbivore performance under elevated CO₂ is associated with lower plant defence signalling and minimal declines in nutritional quality. *Scientific Reports* **10**, 14553.
- Katabuchi M.** 2015. LeafArea: an R package for rapid digital analysis of leaf area. *Ecological Research* **30**, 1073–1077.
- Kattge J, Knorr W, Raddatz T, Wirth C.** 2009. Quantifying photosynthetic capacity and its relationship to leaf nitrogen content for global-scale terrestrial biosphere models. *Global Change Biology* **15**, 976–991.
- Kenward MG, Roger JH.** 1997. Small sample inference for fixed effects from restricted maximum likelihood. *Biometrics* **53**, 983–997.
- Kou-Giesbrecht S, Arora VK, Seiler C, et al.** 2023. Evaluating nitrogen cycling in terrestrial biosphere models: a disconnect between the carbon and nitrogen cycles. *Earth System Dynamics* **14**, 767–795.
- LeBauer DS, Treseder KK.** 2008. Nitrogen limitation of net primary productivity in terrestrial ecosystems is globally distributed. *Ecology* **89**, 371–379.
- Lee TD, Barrott SH, Reich PB.** 2011. Photosynthetic responses of 13 grassland species across 11 years of free-air CO₂ enrichment is modest, consistent and independent of N supply. *Global Change Biology* **17**, 2893–2904.
- Lenth R.** 2019. emmeans: estimated marginal means, aka least-squares means. <https://cran.r-project.org/package=emmeans>
- Liang J, Qi X, Souza L, Luo Y.** 2016. Processes regulating progressive nitrogen limitation under elevated carbon dioxide: a meta-analysis. *Biogeosciences* **13**, 2689–2699.
- Lu J, Yang J, Keitel C, Yin L, Wang P, Cheng W, Dijkstra FA.** 2022. Belowground carbon efficiency for nitrogen and phosphorus acquisition varies between *Lolium perenne* and *Trifolium repens* and depends on phosphorus fertilization. *Frontiers in Plant Science* **13**, 927435.
- Luo X, Keenan TF, Chen JM, et al.** 2021. Global variation in the fraction of leaf nitrogen allocated to photosynthesis. *Nature Communications* **12**, 4866.
- Luo Y, Currie WS, Dukes JS, et al.** 2004. Progressive nitrogen limitation of ecosystem responses to rising atmospheric carbon dioxide. *BioScience* **54**, 731–739.
- Luo Y, Field CB, Mooney HA.** 1994. Predicting responses of photosynthesis and root fraction to elevated [CO₂]: interactions among carbon, nitrogen, and growth. *Plant, Cell & Environment* **17**, 1195–1204.
- Maire V, Martre P, Kattge J, Gastal F, Esser G, Fontaine S, Soussana J-F.** 2012. The coordination of leaf photosynthesis links C and N fluxes in C₃ plant species. *PLoS One* **7**, e38345.
- Makino A, Harada M, Sato T, Nakano H, Mae T.** 1997. Growth and N allocation in rice plants under CO₂ enrichment. *Plant Physiology* **115**, 199–203.
- McCulloch LA, Porder S.** 2021. Light fuels while nitrogen suppresses symbiotic nitrogen fixation hotspots in neotropical canopy gap seedlings. *New Phytologist* **231**, 1734–1745.
- Medlyn BE, Badeck FW, De Pury DGG, et al.** 1999. Effects of elevated [CO₂] on photosynthesis in European forest species: a meta-analysis of model parameters. *Plant, Cell & Environment* **22**, 1475–1495.
- Meyerholt J, Sickel K, Zaehle S.** 2020. Ensemble projections elucidate effects of uncertainty in terrestrial nitrogen limitation on future carbon uptake. *Global Change Biology* **26**, 3978–3996.
- Moore DJP, Aref S, Ho RM, Phipps JS, Hamilton JG, De Lucia EH.** 2006. Annual basal area increment and growth duration of *Pinus taeda* in response to eight years of free-air carbon dioxide enrichment. *Global Change Biology* **12**, 1367–1377.
- Nakano H, Makino A, Mae T.** 1997. The effect of elevated partial pressures of CO₂ on the relationship between photosynthetic capacity and N content in rice leaves. *Plant Physiology* **115**, 191–198.
- Nie M, Lu M, Bell J, Raut S, Pendall E.** 2013. Altered root traits due to elevated CO₂: a meta-analysis. *Global Ecology and Biogeography* **22**, 1095–1105.
- Niinemets U, Tenhunen JD.** 1997. A model separating leaf structural and physiological effects on carbon gain along light gradients for the shade-tolerant species *Acer saccharum*. *Plant, Cell & Environment* **20**, 845–866.
- Norby RJ, Warren JM, Iversen CM, Medlyn BE, McMurtrie RE.** 2010. CO₂ enhancement of forest productivity constrained by limited nitrogen availability. *Proceedings of the National Academy of Sciences, USA* **107**, 19368–19373.
- Nowak RS, Ellsworth DS, Smith SD.** 2004. Functional responses of plants to elevated atmospheric CO₂—do photosynthetic and productivity data from FACE experiments support early predictions? *New Phytologist* **162**, 253–280.
- Onoda Y, Wright IJ, Evans JR, Hikosaka K, Kitajima K, Niinemets U, Poorter H, Tosens T, Westoby M.** 2017. Physiological and structural tradeoffs underlying the leaf economics spectrum. *New Phytologist* **214**, 1447–1463.
- Pastore MA, Lee TD, Hobbie SE, Reich PB.** 2019. Strong photosynthetic acclimation and enhanced water-use efficiency in grassland functional groups persist over 21 years of CO₂ enrichment, independent of nitrogen supply. *Global Change Biology* **25**, 3031–3044.
- Peng Y, Prentice IC, Bloomfield KJ, Campioli M, Guo Z, Sun Y, Tian D, Wang X, Vicca S, Stocker BD.** 2023. Global terrestrial nitrogen uptake and nitrogen use efficiency. *Journal of Ecology* **111**, 2676–2693.
- Perkowski EA, Ezekannagha E, Smith NG.** 2025. Dataset and analysis code for: Nitrogen demand, supply, and acquisition strategy control plant responses to elevated CO₂ at different scales. Zenodo. doi: [10.5281/zenodo.14962595](https://doi.org/10.5281/zenodo.14962595)

- Perkowski EA, Terrones J, German HL, Smith NG.** 2024. Symbiotic nitrogen fixation reduces belowground biomass carbon costs of nitrogen acquisition under low, but not high, nitrogen availability. *AoB Plants* **16**, 1–22.
- Perkowski EA, Waring EF, Smith NG.** 2021. Root mass carbon costs to acquire nitrogen are determined by nitrogen and light availability in two species with different nitrogen acquisition strategies. *Journal of Experimental Botany* **72**, 5766–5776.
- Poorter H, Bühler J, Van Dusschoten D, Climent J, Postma JA.** 2012. Pot size matters: a meta-analysis of the effects of rooting volume on plant growth. *Functional Plant Biology* **39**, 839–850.
- Poorter H, Knopf O, Wright IJ, Temme AA, Hogewoning SW, Graf A, Cernusak LA, Pons TL.** 2022. A meta-analysis of responses of C_3 plants to atmospheric CO_2 : dose–response curves for 85 traits ranging from the molecular to the whole-plant level. *New Phytologist* **233**, 1560–1596.
- Prentice IC, Dong N, Gleason SM, Maire V, Wright IJ.** 2014. Balancing the costs of carbon gain and water transport: testing a new theoretical framework for plant functional ecology. *Ecology Letters* **17**, 82–91.
- Prentice IC, Liang X, Medlyn BE, Wang Y-P.** 2015. Reliable, robust and realistic: the three R's of next-generation land-surface modelling. *Atmospheric Chemistry and Physics* **15**, 5987–6005.
- Rastetter EB, Vitousek PM, Field CB, Shaver GR, Herbert D, Ågren GI.** 2001. Resource optimization and symbiotic nitrogen fixation. *Ecosystems* **4**, 369–388.
- R Core Team.** 2021. R: a language and environment for statistical computing. Vienna, Austria: R Foundation for Statistical Computing.
- Reich PB, Hobbie SE, Lee TD, Ellsworth DS, West JB, Tilman D, Knops JMH, Naeem S, Trost J.** 2006. Nitrogen limitation constrains sustainability of ecosystem response to CO_2 . *Nature* **440**, 922–925.
- Rogers A, Ainsworth EA, Leakey ADB.** 2009. Will elevated carbon dioxide concentration amplify the benefits of nitrogen fixation in legumes? *Plant Physiology* **151**, 1009–1016.
- Rogers A, Medlyn BE, Dukes JS, et al.** 2017. A roadmap for improving the representation of photosynthesis in Earth system models. *New Phytologist* **213**, 22–42.
- Saathoff AJ, Welles J.** 2021. Gas exchange measurements in the unsteady state. *Plant, Cell & Environment* **44**, 3509–3523.
- Sage RF.** 1994. Acclimation of photosynthesis to increasing atmospheric CO_2 : the gas exchange perspective. *Photosynthesis Research* **39**, 351–368.
- Schneider CA, Rasband WS, Eliceiri KW.** 2012. NIH Image to ImageJ: 25 years of image analysis. *Nature Methods* **9**, 671–675.
- Sigurdsson BD, Medhurst JL, Wallin G, Eggertsson O, Linder S.** 2013. Growth of mature boreal Norway spruce was not affected by elevated $[CO_2]$ and/or air temperature unless nutrient availability was improved. *Tree Physiology* **33**, 1192–1205.
- Smith NG, Dukes JS.** 2013. Plant respiration and photosynthesis in global-scale models: incorporating acclimation to temperature and CO_2 . *Global Change Biology* **19**, 45–63.
- Smith NG, Keenan TF.** 2020. Mechanisms underlying leaf photosynthetic acclimation to warming and elevated CO_2 as inferred from least-cost optimality theory. *Global Change Biology* **26**, 5202–5216.
- Smith NG, Keenan TF, Prentice IC, et al.** 2019. Global photosynthetic capacity is optimized to the environment. *Ecology Letters* **22**, 506–517.
- Smith NG, Zhu Q, Keenan TF, Riley WJ.** 2024. Acclimation of photosynthesis to CO_2 increases ecosystem carbon storage due to leaf nitrogen savings. *Global Change Biology* **30**, 1–10.
- Smith SE, Read DJ.** 2008. *Mycorrhizal symbiosis*, 3rd edn. Amsterdam: Elsevier.
- Stocker BD, Dong N, Perkowski EA, et al.** 2025. Empirical evidence and theoretical understanding of ecosystem carbon and nitrogen cycle interactions. *New Phytologist* **245**, 49–68.
- Taylor BN, Menge DNL.** 2018. Light regulates tropical symbiotic nitrogen fixation more strongly than soil nitrogen. *Nature Plants* **4**, 655–661.
- Tejera-Nieves M, Seong DY, Reist L, Walker BJ.** 2024. The dynamic assimilation technique measures photosynthetic CO_2 response curves with similar fidelity to steady-state approaches in half the time. *Journal of Experimental Botany* **75**, 2819–2828.
- Terrer C, Vicca S, Hungate BA, Phillips RP, Prentice IC.** 2016. Mycorrhizal association as a primary control of the CO_2 fertilization effect. *Science* **353**, 72–74.
- Terrer C, Vicca S, Stocker BD, Hungate BA, Phillips RP, Reich PB, Finzi AC, Prentice IC.** 2018. Ecosystem responses to elevated CO_2 governed by plant–soil interactions and the cost of nitrogen acquisition. *New Phytologist* **217**, 507–522.
- van Groenigen KJ, Six J, Hungate BA, De Graaff MA, Van Breemen N, Van Kessel C.** 2006. Element interactions limit soil carbon storage. *Proceedings of the National Academy of Sciences, USA* **103**, 6571–6574.
- Vitousek PM, Howarth RW.** 1991. Nitrogen limitation on land and in the sea: how can it occur? *Biogeochemistry* **13**, 87–115.
- Walker AP, Beckerman AP, Gu L, Kattge J, Cernusak LA, Domingues TF, Scales JC, Wohlfahrt G, Wullschlegler SD, Woodward FI.** 2014. The relationship of leaf photosynthetic traits— V_{cmax} and J_{max} —to leaf nitrogen, leaf phosphorus, and specific leaf area: a meta-analysis and modeling study. *Ecology and Evolution* **4**, 3218–3235.
- Wang H, Prentice IC, Keenan TF, Davis TW, Wright IJ, Cornwell WK, Evans BJ, Peng C.** 2017. Towards a universal model for carbon dioxide uptake by plants. *Nature Plants* **3**, 734–741.
- Waring EF, Perkowski EA, Smith NG.** 2023. Soil nitrogen fertilization reduces relative leaf nitrogen allocation to photosynthesis. *Journal of Experimental Botany* **74**, 5166–5180.
- Wellburn AR.** 1994. The spectral determination of chlorophylls a and b, as well as total carotenoids, using various solvents with spectrophotometers of different resolution. *Journal of Plant Physiology* **144**, 307–313.
- Wieder WR, Cleveland CC, Smith WK, Todd-Brown K.** 2015. Future productivity and carbon storage limited by terrestrial nutrient availability. *Nature Geoscience* **8**, 441–444.
- Wright IJ, Reich PB, Westoby M.** 2003. Least-cost input mixtures of water and nitrogen for photosynthesis. *The American Naturalist* **161**, 98–111.
- Zavala JA, Nability PD, DeLucia EH.** 2013. An emerging understanding of mechanisms governing insect herbivory under elevated CO_2 . *Annual Review of Entomology* **58**, 79–97.